Self-Absorption Resonances at the Electron-Cyclotron Harmonics

G. Landauer

IPP 3/60 September 1966

INSTITUT FÜR PLASMAPHYSIK

GARCHING BEI MÜNCHEN

INSTITUT FÜR PLASMAPHYSIK

GARCHING BEI MÜNCHEN

Self-Absorption Resonances at the Electron-Cyclotron Harmonics

G. Landauer

IPP 3/60 September 1966

Die nachstehende Arbeit wurde im Rahmen des Vertrages zwischen dem Institut für Plasmaphysik GmbH und der Europäischen Atomgemeinschaft über die Zusammenarbeit auf dem Gebiete der Plasmaphysik durchgeführt.

IPP 3/60 G. Landauer

Self-Absorption Resonances at the Electron-Cyclotron Harmonics.

September 1967 (in English)

Abstract

Sharp self-absorption resonances at the electron-cyclotron harmonics ($n \approx 4 - 18$) appear in radiation spectra, when the PIG discharge is superimposed by a secondary plasma. This plasma is established by two electrodes which produce a static electric field $E \perp B$. The radiation level ("background"), in which at a frequency $f \approx 10$ GHz the self-absorption resonances could be observed, is rather high. On the contrary, normal cyclotron-harmonic emission spectra of the PIG discharge have low background radiation.

1.) The apparatus

The PIG (Penning) discharge is known to be highly effectiv in the excitation of electron-cyclotron harmonic emission spectra in the microwave region [1,2,3]. The PIG discharge was produced between two cold cathodes at both ends (Tantalum, 80 mm Ø), which are on the same potential, and the stainless steel vacuum chamber which acts as anode (inner diameter 150 mm), Fig. 1. To excite cyclotron-harmonic spectra, typical parameters of the discharge are: Helium pressure $p = 10^{-2} - 10^{-1}$ Torr, voltage $U_1 = 0.5 - 1$ kV, current $I_1 = 1 - 5$ A. The apparatus was equipped with two additional Tantalum electrodes (30 mm Ø) in the middle of the vacuum chamber. The position of these electrodes could be moved radially. The angle of the electrode plane with respect to the magnetic field B was $\vartheta = 0^\circ, 30^\circ$ (Fig. 1). The voltage U_2 which was applied to the middle electrodes creates a static electric field $E \perp B$.

The radiation was received at the fixed frequencies f = 10.15 and 34.0 GHz. The spectra were measured while the magnetic field was increased ($B_{max} \approx 2000$ G). At the lower frequency f = 10.15 GHz the radiation was picked up by a dipole antenna ($E \perp B$) which was located inside the vacuum chamber at r = 5 cm. The antenna for f = 34 GHz was a horn, also mounted inside the vacuum chamber. Both antennas were placed outside the plasma region and were connected to normal superhet receivers, using balanced mixers. The i.f. (30 MHz) was amplified and the rectified signal was written with an x-y recorder.

2.) Normal cyclotron-harmonic emission

Emission lines at the electron-cyclotron harmonics on a relative low background radiation (equivalent temperature $T_e \approx 10^4$ °K) was measured under PIG discharge condition (U_2, $I_2 = 0$), Fig. 2. These spectra correspond to earlier results [1,2,3]. Helium was used, $U_1 \approx 800$ V, $I_1 \approx 1$ A.

3.) Secondary plasma (E⊥B)

When the power supply 2 (Fig. 1) applies a voltage U_2 to the middle electrodes, a current I_2 can be measured if the PIG discharge has cared for preionization. The first experiments were carried out with orientation of the electrode planes ∥ B ($\vartheta = 0^\circ$). Fig. 3 shows the voltage-current-characteristics $U_2 = f(I_2)$ of the secondary plasma. For $I_2 > 1$ A the negative characteristic of an arc is measured. In this region the secondary plasma can be maintained without PIG discharge (U_1, $I_1 = 0$). It is remarkable that the voltage U_2 has higher values for low pressure (where the radiation intensity is high, Figs. 4, 7).

After some time of operation the vacuum chamber was opened. There were melted spots and even burned holes in the PIG cathodes at r,φ -coordinates, which correspond to the position of the negative middle electrode. This and also observation of the plasma through a window suggests the assumption that the current I_2 of the secondary plasma flows ∥ B from one of the middle electrodes to the PIG cathodes and then to the opposite electrode. For this reason the plane of the middle electrodes further was oriented with $\vartheta = 30^\circ$ against the magnetic field lines to avoid excessive current density on the PIG cathodes.

Potential measurements (Fig. 6) show that at currents $I_2 > 1$ A the PIG cathode potential (zero potential in Fig. 6) is between the potential U_{2+} and U_{2-} of the middle electrodes. This behaviour agrees with the observation of current flow from the middle electrodes to the PIG cathodes, which provide a possibility of electron transport ⊥ B due to their conductivity. The PIG voltage U_1 decreases with increasing I_2 to very low values also when I_1 is kept constant ($I_1 \approx 1$ A). The establishment of the secondary plasma and its interaction with the PIG discharge requires further investigation in order to come to a better understanding of the produced plasma.

Nevertheless, the result which is of interest here is that the secondary plasma is highly effective in microwave radiation (f = 10, 15 GHz), which contains a series of self-absorption resonances at the electron-cyclotron harmonics.

4.) Radiation spectra with self-absorption resonances at $\omega \approx n\omega_e$

(ω_e = electron-cyclotron frequency)

Fig. 4 shows radiation diagrams with sharp self-absorption lines for low pressure (20 m Torr). It should be emphasized that there is no external microwave power radiated into the plasma. If the pressure (He) increases the measured absolute intensities decrease and cyclotron-harmonic emission lines tend to appear instead of absorption resonances (Fig. 5). The 50 mTorr curve (Fig. 5) shows clearly that sometimes an emission maximum can be split in two parts by a sharp absorption line (line reversal). The background radiation is rather high compared with PIG operation. The power level of the maximum of the radiation at low pressures (sensitivity of the x-y recorder 0.25 V/cm) in terms of equivalent temperature is $T_e \approx 10^6$ °K. The spectra come out even more clearly for $\vartheta = 30°$. In this case the electrode distance was d = 4 cm, which provided the appearance of a very sharp structure of the self-absorption lines at p = 15; 20 mTorr (Fig. 7). The secondary current I_2 influences the spectra in a sense that only for $I_2 \geqq 2$ A sharp self-absorption appears. At $I_2 \approx 1.0 - 1.5$ A only the 15 mTorr diagram shows absorption. At higher pressure emission lines appear, Fig. 8.

At currents $I_2 > 2$ A the PIG discharge can be switched off without remarkable influence on the secondary plasma and the radiation patterns. Thus it can be concluded that the observed effect of self-absorption resonances is produced by the secondary plasma.

Radiation measurements also have been done at f = 34 GHz. The observed spectra differ in some aspects remarkably from those at 10.15 GHz. At low pressures (20; 30 mTorr), Fig. 9, sharp emission resonances occur at frequencies $\omega \approx n\omega_e$, also when the secondary plasma is burning. The harmonic emission decreases with increasing pressure (Fig. 10) in accordance with earlier observations [1,2,3]. At p = 0.15 Torr the harmonic structure has almost disappeared and the radiation comes out with one distinguished and one or two lower maxima. It is important to note that the received radiation power at f = 34 GHz is approximately by a factor of $10^{-1} - 10^{-2}$ lower than for f = 10.15 GHz.

5.) Discussion

Some earlier measurements showed line reversal of cyclotron-harmonic emission lines, or if the effect is small a "dip" [4,5,6,7]. The background radiation level in these experiments is low. The experiments, the results of which are presented here and in [8] show clearly that the harmonic radiation can be completely converted into harmonic absorption, provided that the background level is sufficiently high. Though it is not possible at the moment to give a satisfactory description of the phenomenon, it may be understood as analogous to observations of line reversal in the optical frequency region. Following this model we may assume that the produced plasma has two main regions: one with intense radiation and a second one with resonance absorption at frequencies $\omega \approx n\omega_e$. Let us assume for example a hot core and an absorbing shell around. When the radiation of the hot core crosses the shell, the radiation is subdue to harmonic absorption. Without the hot core it should be possible to receive low level harmonic emission lines from the proposed outer shell. Harmonic emission lines without absorption resonances may be expected also from the hot region, if there is no absorbing shell. Most of the diagrams (Figs. 4, 5, 7) show a very abrupt change from emission to absorption resonance, which is due to the difference in line width of emission and absorption. The small peaks at the bottom of some absorption lines (n = 6 - 12, p = 15; 20 mTorr, Fig. 7) may perhaps be interpreted as peaks of emission from the shell. In the view of this model the outer plasma shell is resonance heated at $\omega \approx n\omega_e$ from the hot center. However, the assumption of two different plasma regions, as discussed before, seems to be not necessary if one assumes a plasma with an electron velocity distribution which has at least two distinguished groups of electrons, one responsible for the high power radiation, the other for the harmonic absorption.

The high level radiation may have any non-thermal origin with particularly high excitation at frequencies $f \approx 10$ GHz. The excitation at $f \approx 34$ GHz is considerably lower. The non-thermal character of the radiation is emphasized by the fact that low frequency oscillations of high intensity, which superimpose the d. c. voltages and currents of both plasmas, indicate the existence of instabili-

ties. Usually the high level radiation has one significant maximum with dependence on the magnetic field. Fig. 10 shows that this maximum (and also the lower maxima in this diagram) is shifted to higher B (lower ω/ω_e) when the secondary current decreases.

Acknowledgements

The author thanks Dipl.-Ing. F. Leuterer and Dr. D. Pfirsch for valuable discussions.

References

1 G. Landauer: V. Int. Conf. on Phen. in Ionized Gases, München, 1961. North Holland Publ. Co., Amsterdam, 1, 389.

2 G. Landauer: J. Nucl. Energy, Pt. C, 4, 1962, 395

3 H. Dreicer: Proc. VII. Int. Conf. on Phen. in Ionized Gases, Belgrade, 1965, 491

4 S. Tanaka, H. Kubo: IPPJ-23 (1964)

5 C.D. Lustig: Phys. Rev. Vol. 139 (1965), A 63

6 E. Canobbio, T. Consoli et al.: Proc. VII. Int. Conf. on Phen. in Ionized Gases, Belgrade, 1965, 516

7 H. Ikegami, F.W. Crawford: Proc. VII. Int. Conf. on Phen. in Ionized Gases, Belgrade, 1965, 503

8 G. Landauer: Phys. Let. (to be published in Oct. 1967)

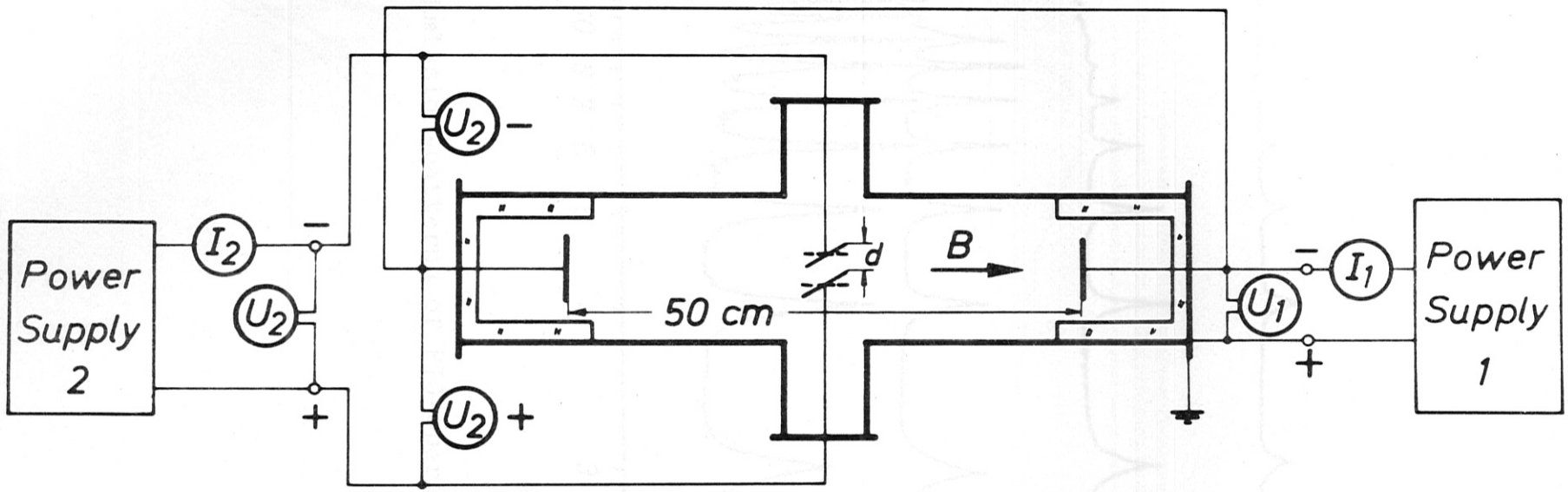

Fig 1. PIG-discharge with E ⊥ B-electrodes in the middle.

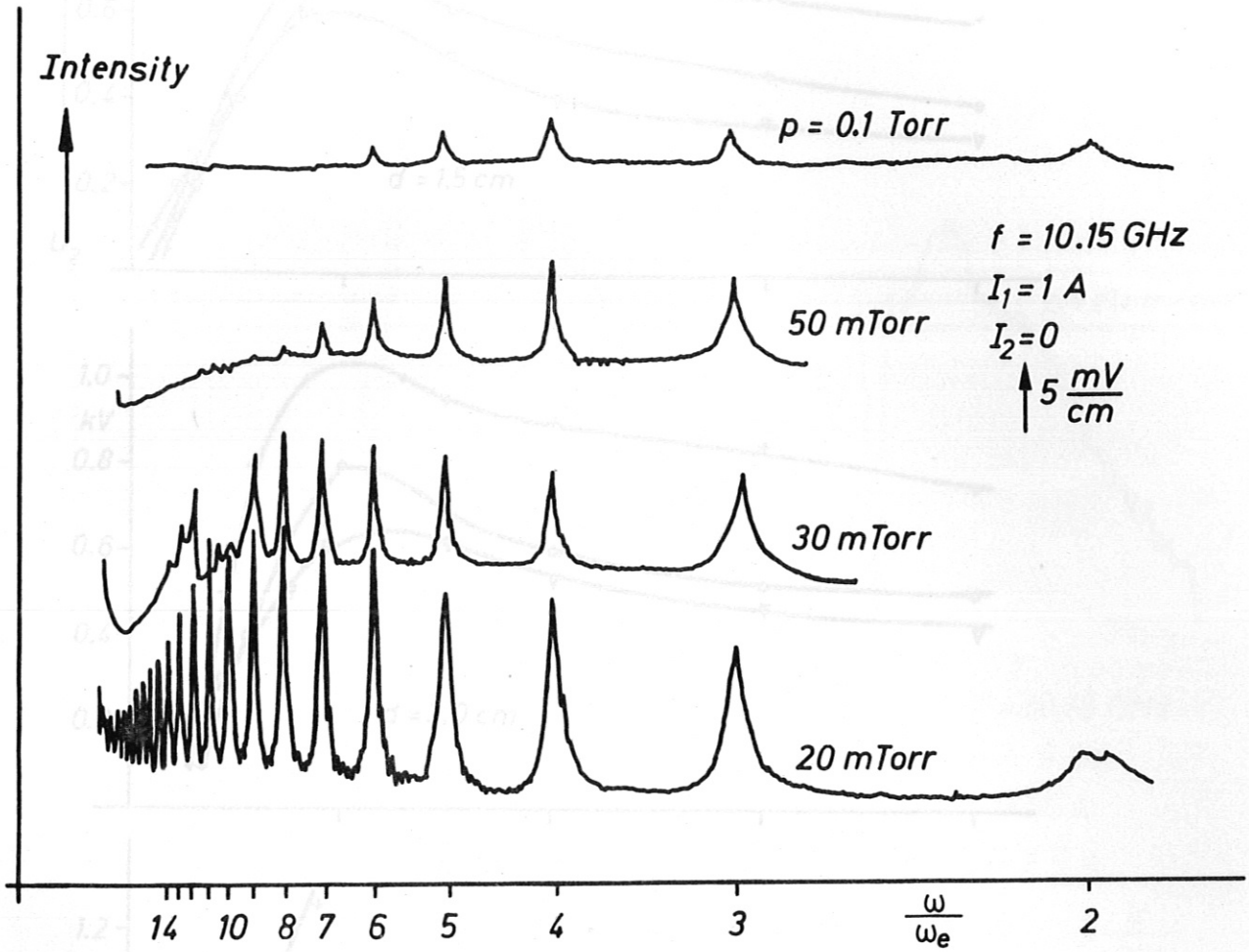

Fig 2. Emission-patterns of PIG-operation ($I_2 = 0$).

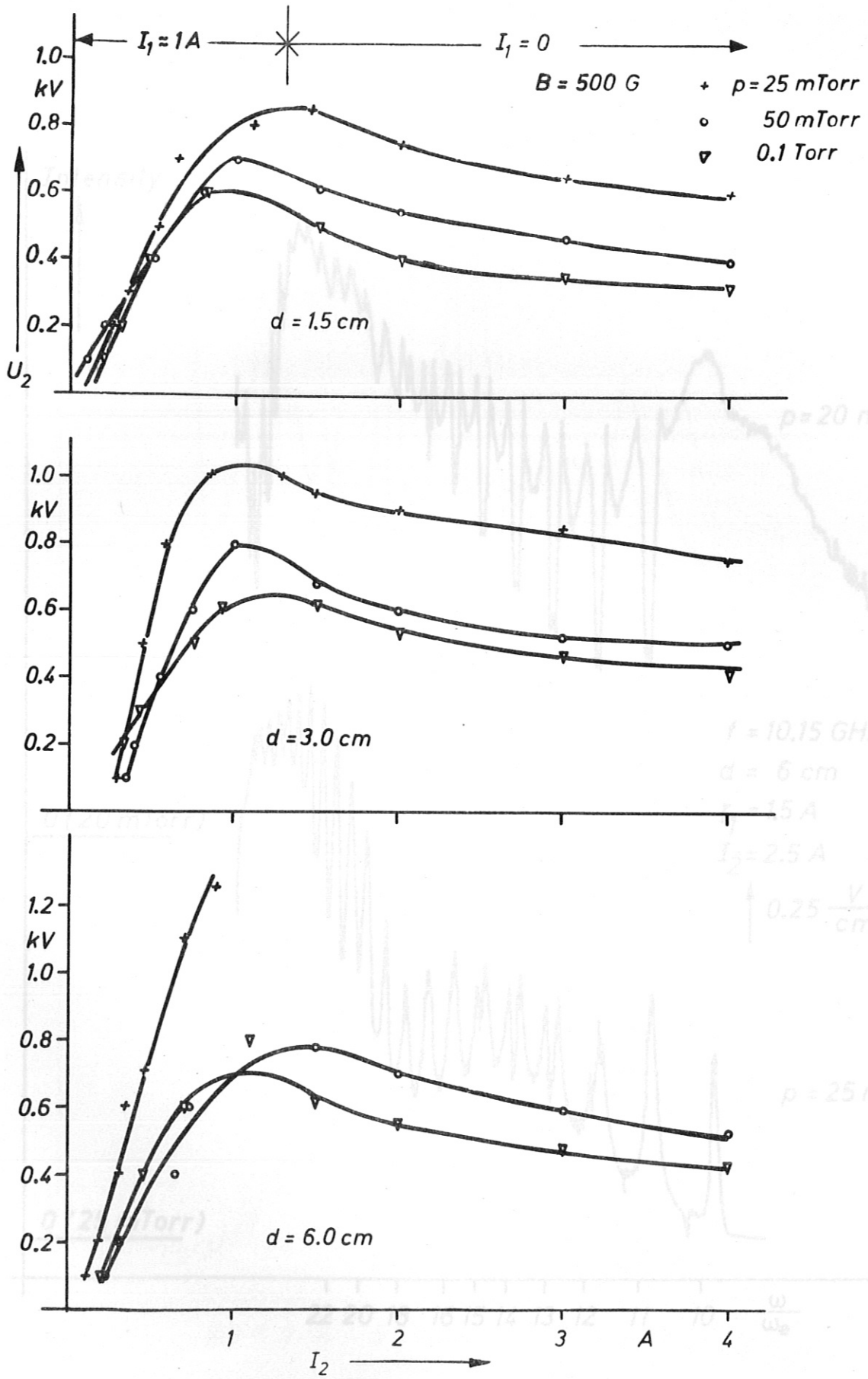

Fig 3. Voltage-current-characteristic of the E⊥B-discharge (secondary plasma), $\vartheta = 0°$.

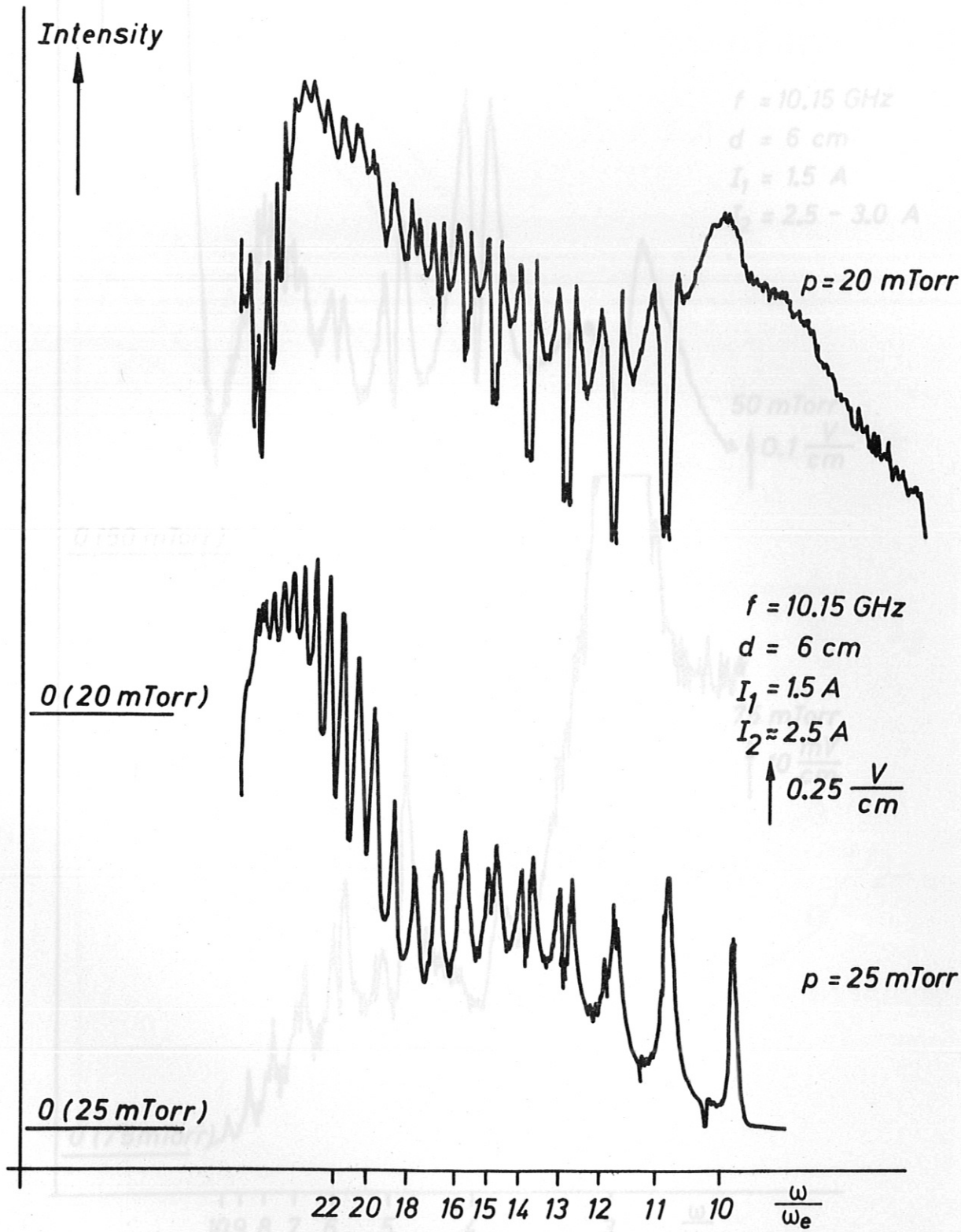

Fig 4. Emission-patterns of E⊥B-discharge, $\vartheta = 0^\circ$, d = 6 cm.

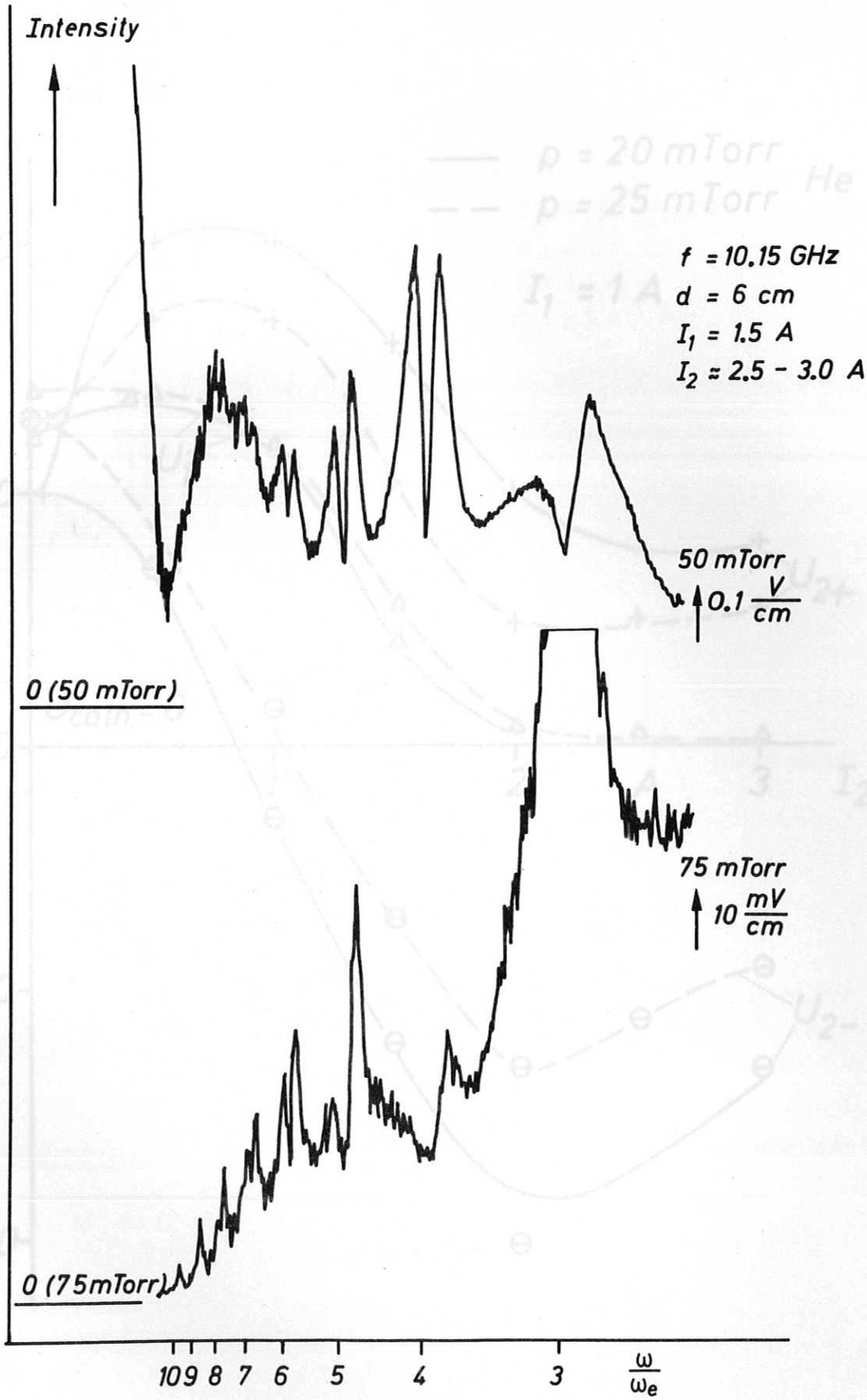

Fig 5. Emission-patterns of E⊥B-discharge, $\vartheta = 0°$, d = 6 cm.

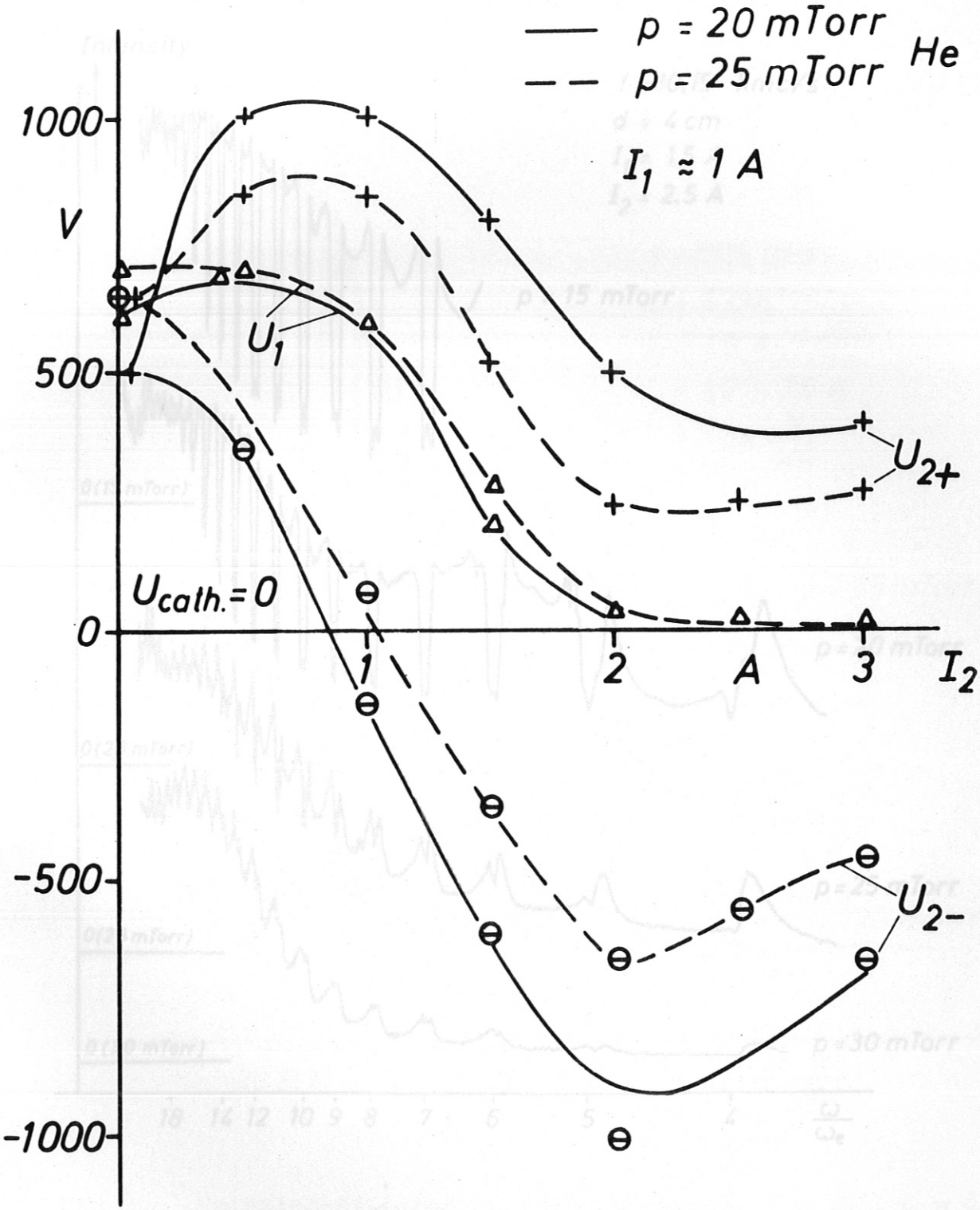

Fig.6. Electrode potentials, $\vartheta = 30^{\circ}$.

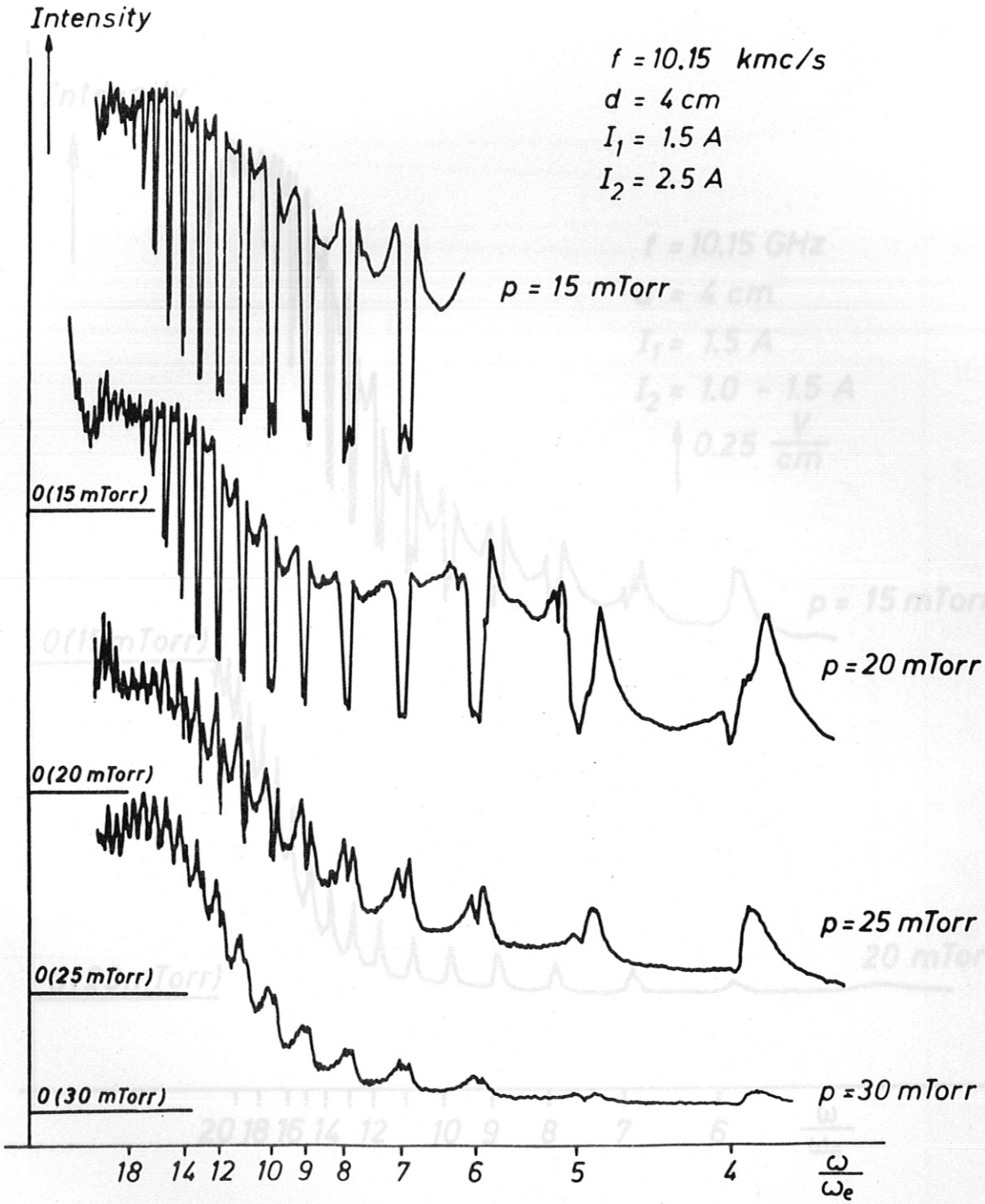

Fig 7. Emission-patterns of E⊥B-discharge, $\vartheta = 30^\circ$, d = 4 cm.

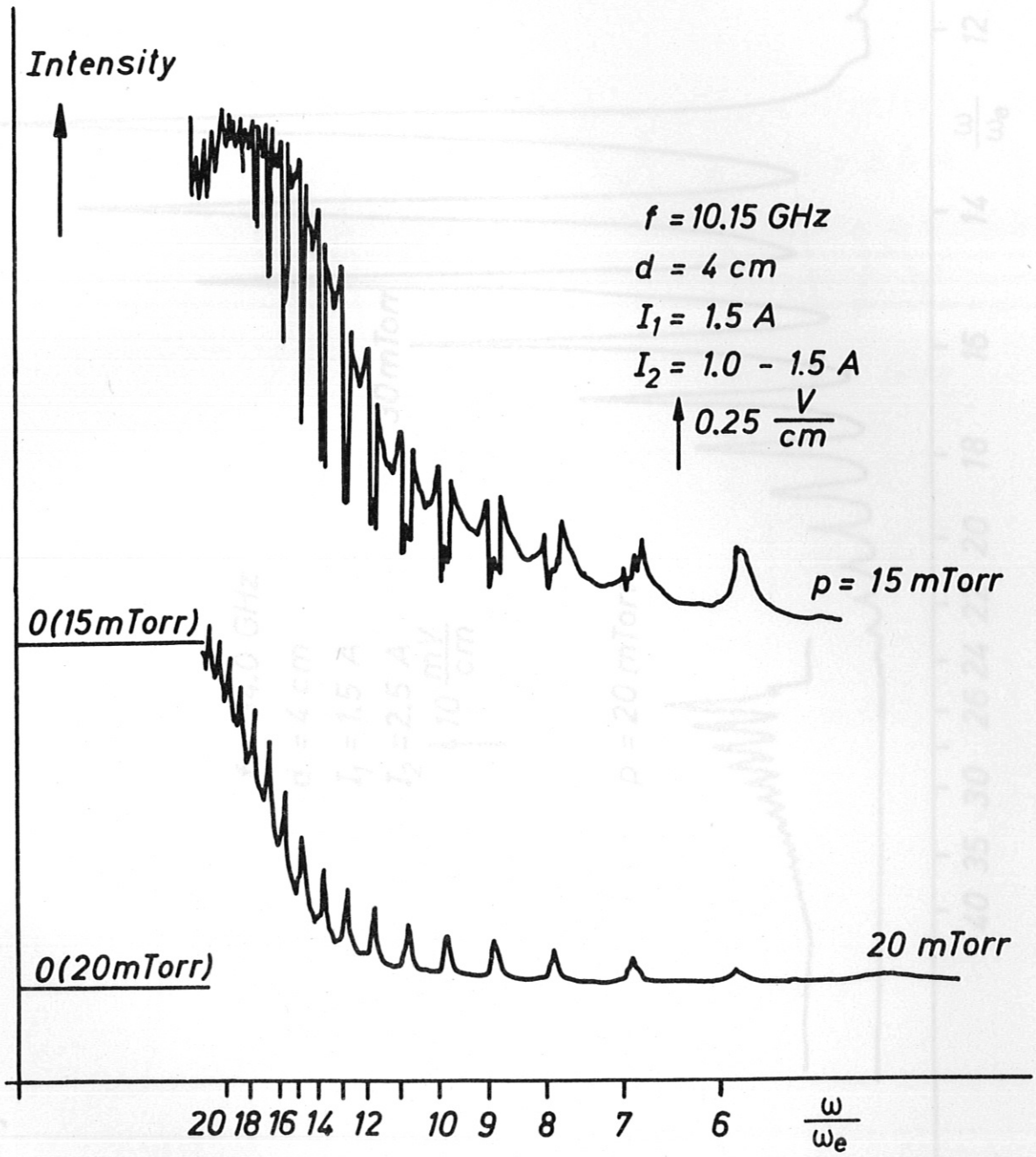

Fig 8. Emission-patterns of E ⊥ B-discharge, $\vartheta = 30°$, d = 4 cm.

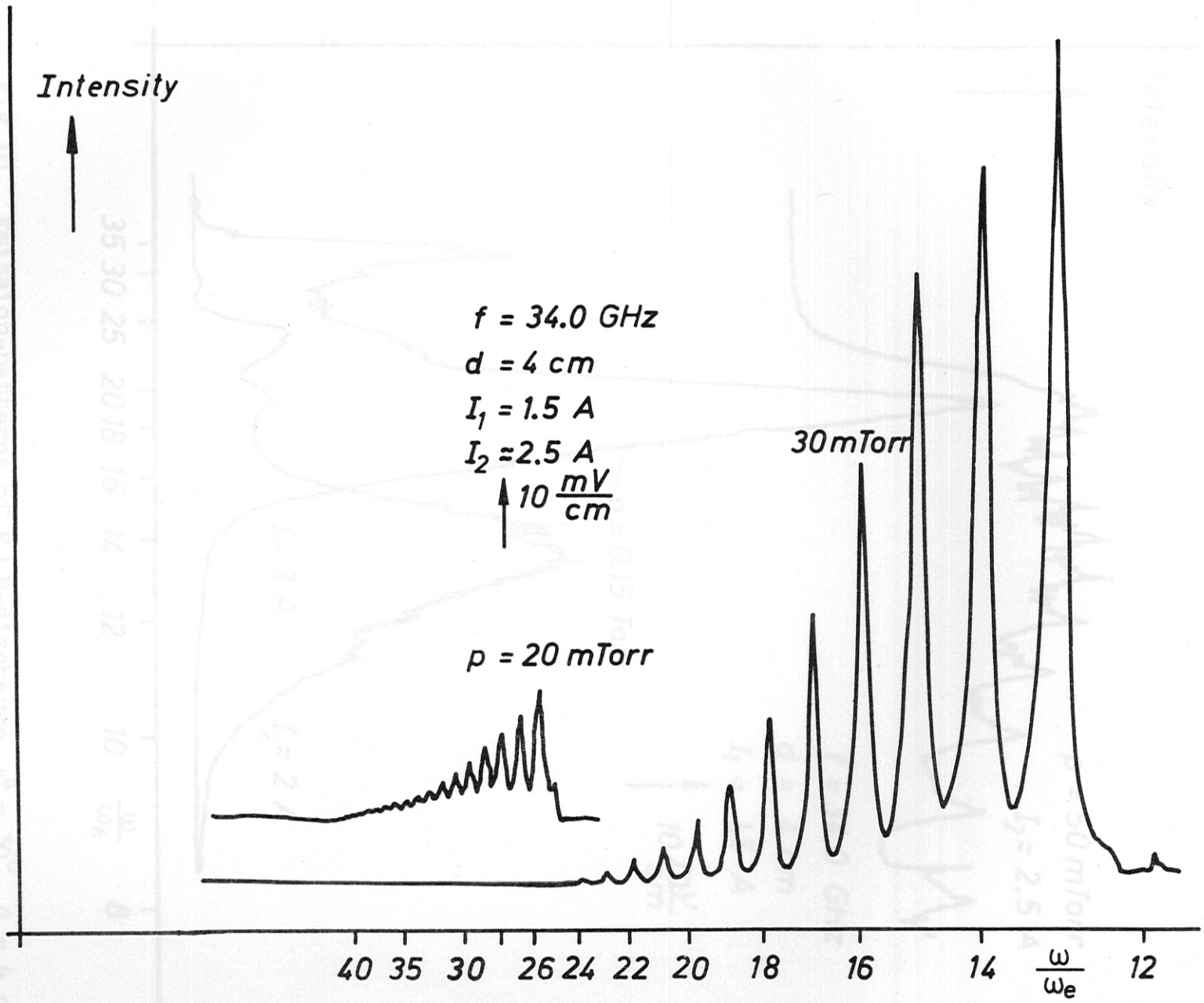

Fig 9. Emission-patterns of E ⊥ B-discharge, $\vartheta = 30°$, d = 4 cm.

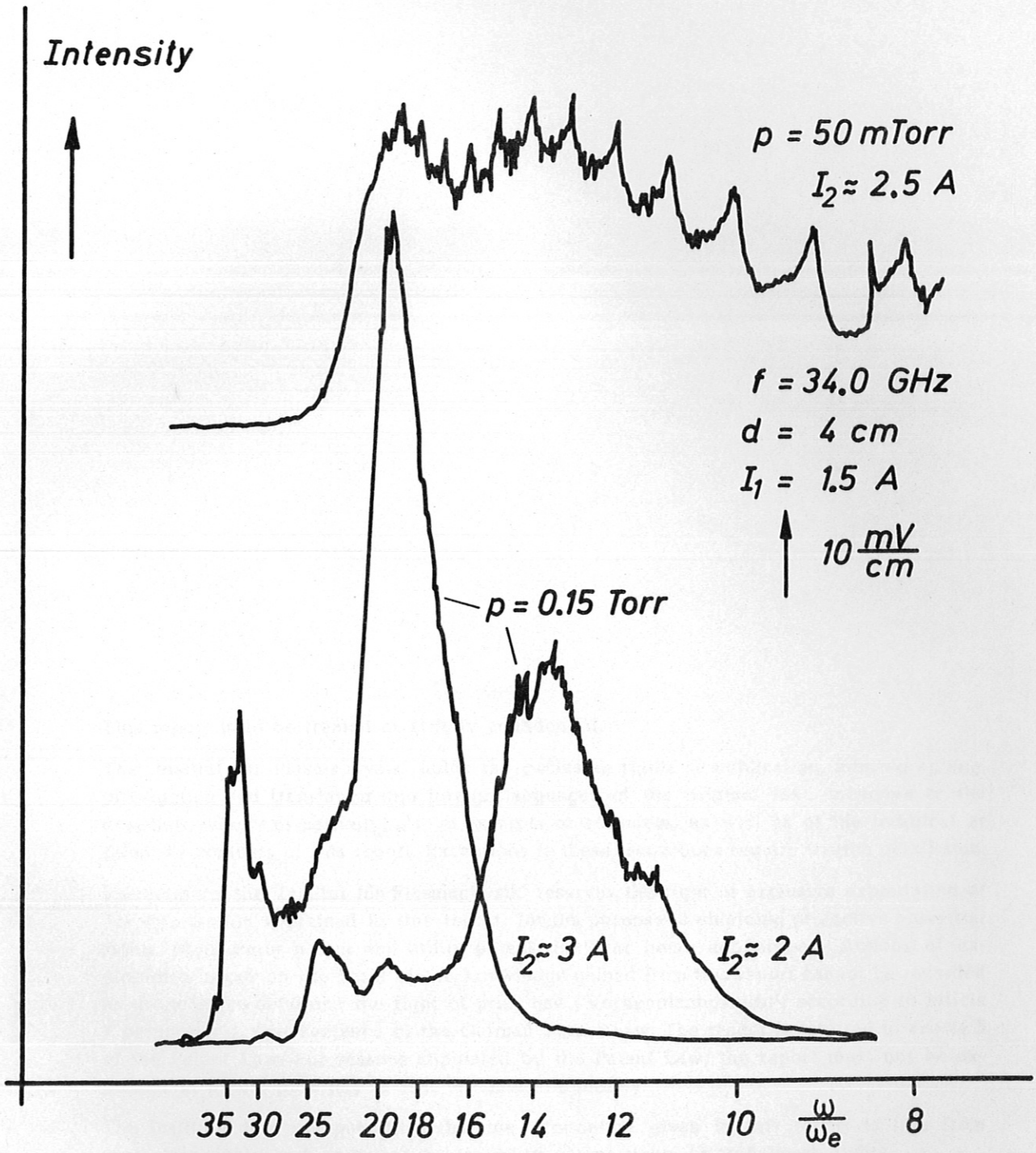

Fig 10. Emission-patterns of E⊥B-discharge, $\vartheta = 30^\circ$, d = 4 cm.